

***P*-Chiral Tetrachosphine Dirhodium Complex as a Catalyst for Asymmetric Hydrogenation: Synthesis, Structure, Enantioselectivity, and Mechanism. Stereoselective Formation of a Dirhodium Tetrahydride Complex and Its Reaction with Methyl (*Z*)- α -Acetamidocinnamate**

Tsuneo Imamoto,^{*,†} Keiji Yashio,[†] Karen V. L. Crépy,[†] Kosuke Katagiri,[†]
Hidetoshi Takahashi,[†] Mitsuhiro Kouchi,[‡] and Ilya D. Gridnev^{*,‡}

Department of Chemistry, Faculty of Science, Chiba University, Yayoi-cho, Inage-ku,
Chiba 263-8522, Japan, and COE Laboratory, Department of Chemistry, Graduate School of Science,
Tohoku University, Sendai 980-8578, Japan

Received September 2, 2005

Optically active C_2 -symmetric tetrachosphine **4** was prepared via the phosphine-borane methodology. Its dirhodium complex **5** was structurally characterized and probed as a catalyst in asymmetric hydrogenations of representative prochiral substrates, demonstrating high activity and good to excellent enantioselectivities. A mechanistic study revealed that **5** can be cleanly and stereoselectively converted to the tetrahydride species **6a**, which is stable up to 0 °C and at higher temperatures slowly decomposes without the loss of hydrogen. The low-temperature (–80 °C) reaction of **6a** with methyl (*Z*)- α -acetamidocinnamate (MAC) cleanly gave the tetrahydride complex **7** containing one molecule of the substrate coordinated only via the amidocarbonyl group, whereas the double bond of the substrate remained noncoordinated. Raising the temperature to –40 °C resulted in irreversible isomerization of complex **7** to **8**, which differs from **7** only by the spatial arrangement of ligands. Migratory insertion proceeding simultaneously with the isomerization of **7** to **8** yields the trihydride complex **9**, which is an analogue of the monohydride intermediates described previously. When the reaction of **6a** with MAC was carried out in the presence of an excess of MAC, the released dirhodium complex was captured by the substrate to give the catalyst–substrate complex **10**, which was characterized by multinuclear NMR. Substrate MAC is much more loosely bound in octahedral complexes **7** and **8** than in the square planar catalyst–substrate complex **10**. This finding provides experimental support for the stereoselection during the association step of the Rh-catalyzed asymmetric hydrogenation.

Introduction

Advances in the Rh-catalyzed asymmetric hydrogenation of prochiral activated olefins are well recognized academically¹ and requested by the pharmaceutical industry.² Further research in this area will lead to the creation of still more effective and enantioselective catalysts, and ultimately to rational ligand

design based on detailed knowledge of the intricate catalytic cycle and the mechanism of stereoselection.

In the past decade *P*-stereogenic diphosphine ligands have played a pivotal role in the creation of a strictly defined asymmetric environment around the metal center.³ On the other hand, the almost exclusive importance of C_2 -symmetric diphosphines has been undermined by successful use of chiral monophosphines⁴ or C_1 -symmetric diphosphines⁵ with only one stereogenic center in the ligand. A further extension of the structural variety of the rhodium-phosphine complexes would be the synthesis of polymetallic complexes, since one could be interested in studying the cooperative effects of several identical

* To whom correspondence should be addressed. (T.I.) Phone/fax: +81 (0)43 290 2791. E-mail: imamoto@faculty.chiba-u.jp. (I.D.G.) Phone: +81 (0)22 795 3585. Fax: +81 (0)22 795 6784. E-mail: igradnev@mail.tains.tohoku.ac.jp.

[†] Chiba University.

[‡] Tohoku University.

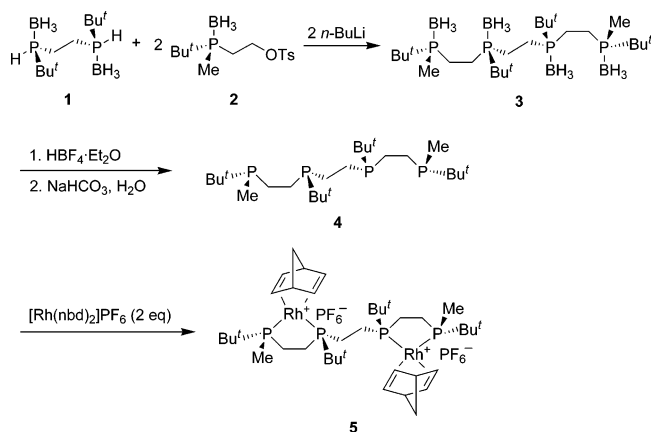
(1) For representative reviews, see: (a) Chi, Y.; Tang, W.; Zhang, X. In *Modern Rhodium-Catalyzed Organic Reactions*; Evans, P. A., Ed.; Wiley-VCH: Weinheim, 2005; pp 1–31. (b) Knowles, W. S. *Angew. Chem., Int. Ed.* **2002**, *41*, 1998. (c) Noyori, R. *Angew. Chem., Int. Ed.* **2002**, *41*, 2008. (d) Tang, W.; Zhang, X. *Chem. Rev.* **2003**, *103*, 3029. (e) Genet, J.-P. *Acc. Chem. Res.* **2003**, *36*, 908. (f) RajanBabu, T. V.; Yan, Y.-Y.; Shin, S. *Curr. Org. Chem.* **2003**, *7*, 1759. (g) Ohkuma, T.; Kitamura, M.; Noyori, R. In *Catalytic Asymmetric Synthesis*, 2nd ed.; Ojima, I., Ed.; Wiley-VCH: New York, 2000; pp 1–110. (h) Brown, J. M. In *Comprehensive Asymmetric Catalysis*; Jacobsen, E. N., Pfalz, A., Yamamoto, H., Eds.; Springer-Verlag: Berlin, 1999; Vol. I, pp 121–182.

(2) For representative reviews, see: (a) Cobley, C. J.; Johnson, N. B.; Lennon, I. C.; McCague, R.; Ramsden, J. A.; Zanotti-Gerosa, A. In *Asymmetric Catalysis on Industrial Scale*; Blaser, H.-U., Schmidt, E., Eds.; Wiley-VCH: Weinheim, 2004; pp 269–282. (b) Sumi, K.; Kumobayashi, H. *Top. Organomet. Chem.* **2004**, *6*, 63.

(3) Reviews: (a) Crépy, K. V. L.; Imamoto, T. *Top. Curr. Chem.* **2003**, *229*, 1. (b) Crépy, K. V. L.; Imamoto, T. *Adv. Synth. Catal.* **2003**, *345*, 79. (c) Pietrusiewicz, K. M.; Zablocka, M. *Chem. Rev.* **1994**, *94*, 1375.

(4) (a) Guillen, F.; Fiaud, J.-C. *Tetrahedron Lett.* **1999**, *40*, 2939. (b) Claver, C.; Fernandez, E.; Gillon, A.; Heslop, K.; Hyett, D. J.; Martorell, A.; Orpen, A. G.; Pringle, P. G. *Chem. Commun.* **2000**, 961. (c) Reetz, M. T.; Mehler, G. *Angew. Chem., Int. Ed.* **2000**, *39*, 3889. (d) van den Berg, M.; Minnaard, A. J.; Schudde, E. P.; van Esch, J.; de Vries, A. H. M.; de Vries, J. G.; Feringa, B. L. *J. Am. Chem. Soc.* **2000**, *122*, 11539. (e) Komarov, I. V.; Börner, A. *Angew. Chem., Int. Ed.* **2001**, *40*, 1197. (f) Ostermeier, M.; Priess, J.; Helmchen, G. *Angew. Chem., Int. Ed.* **2002**, *41*, 612. (g) Hu, A.-G.; Fu, Y.; Xie, J.-H.; Zhou, H.; Wang, L.-X.; Zhou, Q.-L. *Angew. Chem., Int. Ed.* **2002**, *41*, 2348. (h) Jia, X.; Guo, R.; Li, X.; Yao, X.; Chan, A. S. C. *Tetrahedron Lett.* **2002**, *43*, 5541. (i) Agbassou-Niedercorn, F.; Suisse, I. *Coord. Chem. Rev.* **2003**, *242*, 145. (j) Jerphagnon, T.; Renaud, J.-L.; Bruneau, C. *Tetrahedron: Asymmetry* **2004**, *15*, 2101.

Scheme 1. Synthesis of Dirhodium Complex 5



catalytic centers in these highly effective asymmetric catalysts,⁶ which is important for the development of recoverable polymer-supported and dendrimeric catalysts.⁷

Here we report the synthesis and crystal structure of the dirhodium complex of a new *P*-stereogenic tetraphosphine ligand combining two 1,2-bis(alkylmethylphosphino)ethane (BisP*)-like units in one molecule. It is also reported that this complex demonstrates excellent enantioselectivity of asymmetric hydrogenation of representative prochiral substrates. The mechanistic details of the asymmetric hydrogenation catalyzed by this dirhodium complex revealed by an in-depth NMR study are also described.

Results and Discussion

Synthesis and Structure of the Dirhodium Complex. We used the well-developed chemistry of air-stable phosphine-boranes⁸ for the synthesis of a new tetraphosphine ligand (Scheme 1). Thus, secondary phosphine-borane **1**⁹ was reacted with 2 equiv of tosylate **2**¹⁰ to give a single enantiomer of the tetraphosphine-borane **3** with a 65% yield. Deprotection of **3** by treatment with tetrafluoroboric acid¹¹ afforded the desired

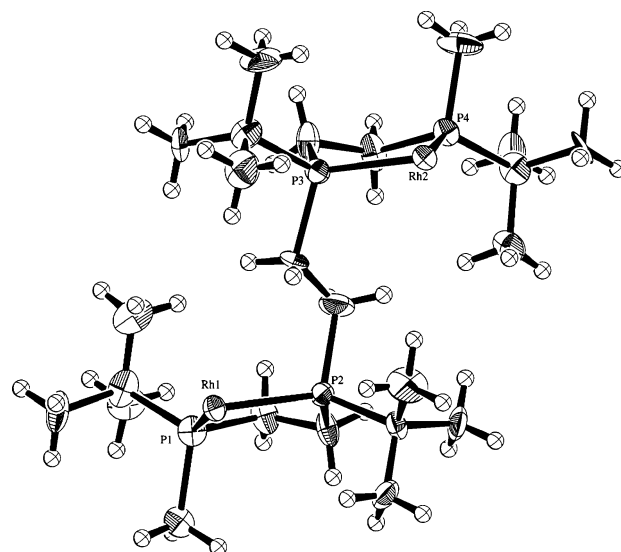


Figure 1. Molecular structure (30% thermal ellipsoids) of complex **5**. The two norbornadiene ligands and the two PF_6^- anions are omitted for clarity.

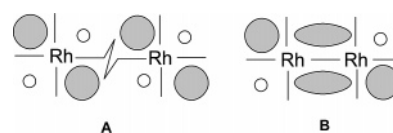


Figure 2. Two different quadrant diagrams conceivable for the dirhodium complex **5**.

tetraphosphine **4**, which was subjected to complexation with 2 equiv of $[\text{Rh}(\text{nbd})_2]\text{PF}_6$ to furnish Rh complex **5**.

The X-ray structure of the dirhodium complex **5** shown in Figure 1 gives important hints on the exact nature of the asymmetric environment around the rhodium atoms in **5**. Formally, the bridging ethylene group might be regarded as a small substituent, similar to a methyl group. In this case the quadrant diagram for **5** consists of two independent units (Figure 2, **A**), each looking like a quadrant diagram for a *t*-Bu-BisP* rhodium complex.¹² On the other hand, the single-crystal X-ray structure of **5** (Figure 1) suggests that two *t*-Bu groups and the bridging ethylene group may provide sufficient hindrance to preclude the formation of a chelate ring inside the molecule. This kind of asymmetric environment corresponds to another type of quadrant diagram (Figure 2, **B**) resembling that recently reported for the “threechickenfootphos” ligand.^{5a} Further experimental results (vide infra) suggest that the quadrant diagram of type **B** (Figure 2) is operative in the Rh-catalyzed asymmetric hydrogenation.

Asymmetric Hydrogenation Catalyzed by Dirhodium Complex 5. The results of the asymmetric hydrogenation of representative substrates using the dirhodium complex **5** as a catalyst are summarized in Table 1. Excellent results comparable to *t*-Bu-BisP* rhodium complex were obtained for α -dehydroamino acids (entries 1, 2),^{12a} enamides (entries 5–7),¹³ (*E*)- β -dehydroamino acid (entry 8),¹⁴ α,β -unsaturated phosphonate

(5) (a) Hoge, G.; Wu, H.-P.; Kissel, W. S.; Pflum, D. A.; Greene, D. J.; Bao, J. *J. Am. Chem. Soc.* **2004**, *126*, 5966. (b) Wu, H.-P.; Hoge, G. *Org. Lett.* **2004**, *6*, 3645. (c) Blaser, H.; Brieden, W.; Pugin, B.; Spindler, F.; Studer, M.; Togni, A. *Top. Catal.* **2002**, *19*, 3. (d) Ohashi, A.; Imamoto, T. *Org. Lett.* **2001**, *3*, 373. (e) Ohashi, A.; Kikuchi, S.; Yasutake, M.; Imamoto, T. *Eur. J. Org. Chem.* **2002**, *15*, 2535. (f) Matsumura, K.; Shimizu, H.; Saito, T.; Kumobayashi, H. *Adv. Synth. Catal.* **2003**, *345*, 180.

(6) (a) Broussard, M. E.; Juma, B.; Train, S. G.; Peng, W. J.; Laneman, S. A.; Stanley, G. G. *Science* **1993**, *260*, 1784. (b) Matthews, R. C.; Howell, D. K.; Peng, W.-J.; Train, S. G.; Treleaven, W. D.; Stanley, G. G. *Angew. Chem., Int. Ed. Engl.* **1996**, *35*, 2253. (c) Peng, W.-J.; Train, S. G.; Howell, D. K.; Fronczek, F. R.; Stanley, G. G. *Chem. Commun.* **1996**, 2607. (d) Aubry, D. A.; Bridges, N. N.; Ezell, K.; Stanley, G. G. *J. Am. Chem. Soc.* **2003**, *125*, 11180. (e) Hunt, C., Jr.; Fronczek, F. R.; Billodeaux, D. R.; Stanley, G. G. *Inorg. Chem.* **2001**, *40*, 5192. (f) Bowyer, P. K.; Cook, V. C.; Gharib-Naseri, N.; Gugger, P. A.; Rae, A. D.; Swieger, G. F.; Willis, A. C.; Zank, J.; Zank, J.; Wilds, S. B. *Proc. Natl. Acad. Sci.* **2002**, *99*, 4877. (g) Bautista, M. T.; Earl, K. A.; Maltby, P. A.; Morris, R. H. *J. Am. Chem. Soc.* **1988**, *110*, 4056.

(7) (a) Kollner, C.; Pugin, B.; Togni, A. *J. Am. Chem. Soc.* **1998**, *120*, 10274. (b) Kollner, C.; Togni, A. *Can. J. Chem.* **2001**, *79*, 1762. (c) *Chiral Catalyst Immobilization and Recycling*; De Vos, D. E., Vankelecom, I. F. J., Jacobs, P. A., Eds.; Wiley-VCH: Weinheim, 2000.

(8) (a) Imamoto, T.; Oshiki, T.; Onozawa, T.; Kusumoto, T.; Sato, K. *J. Am. Chem. Soc.* **1990**, *112*, 5244. (b) Imamoto, T. *Pure Appl. Chem.* **1993**, *65*, 655.

(9) (a) Miura, T.; Yamada, H.; Kikuchi, S.; Imamoto, T. *J. Org. Chem.* **2000**, *65*, 1877. (b) Nagata, K.; Matsukawa, S.; Imamoto, T. *J. Org. Chem.* **2000**, *65*, 4185. (c) Crépy, K. V. L.; Imamoto, T. *Tetrahedron Lett.* **2002**, *43*, 7735.

(10) Ohashi, A.; Imamoto, T. *Tetrahedron Lett.* **2001**, *42*, 1099.

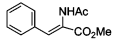
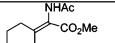
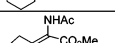
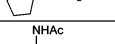
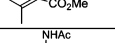
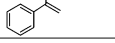
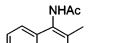
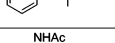
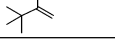
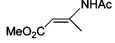
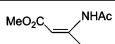
(11) (a) McKinstry, L.; Livinghouse, T. *Tetrahedron Lett.* **1994**, *35*, 9319. (b) McKinstry, L.; Livinghouse, T. *Tetrahedron* **1994**, *50*, 6145.

(12) (a) Imamoto, T.; Watanabe, J.; Wada, Y.; Masuda, H.; Yamada, H.; Tsuruta, H.; Matsukawa, S.; Yamaguchi, K. *J. Am. Chem. Soc.* **1998**, *120*, 1635. (b) Gridnev, I. D.; Higashi, N.; Asakura, K.; Imamoto, T. *J. Am. Chem. Soc.* **2000**, *122*, 7183.

(13) Gridnev, I. D.; Yasutake, M.; Higashi, N.; Imamoto, T. *J. Am. Chem. Soc.* **2001**, *123*, 5268.

(14) Yasutake, M.; Gridnev, I. D.; Higashi, N.; Imamoto, T. *Org. Lett.* **2001**, *3*, 1701.

Table 1. Asymmetric Hydrogenation of Representative Prochiral Substrates Using Dirhodium Complex 5

Entry	Substrate	H ₂ , 5 (s/c = 200)		Product	ee (%) ^a
		H ₂ (atm)	rt, MeOH		
1		2	0.5	99 (R)	
2		6	5	80 (R)	
3		6	5	34 (R)	
4		6	5	37 (R)	
5		2	1	98 (R)	
6		3	12	94 (R)	
7		3	2	99 (S)	
8		3	2	99 (R)	
9		3	12	71 (R)	
10		4	2	81 (S)	
11		2	1	98 (S)	

^a Determined by chiral HPLC and GC.

(entry 9),¹⁵ and dimethyl itaconate (entry 11).^{12a} Modest enantioselectivities were observed only for some β,β -disubstituted α -dehydroamino acids (entries 3, 4)^{12a} and for (*Z*)- β -dehydroamino acid (entry 9).¹⁴

Mechanistic Studies. The mechanism of the rhodium-catalyzed asymmetric hydrogenation has consistently attracted the attention of researchers for over 30 years.^{1,16} Asymmetric hydrogenation is the simplest possible enantioselective catalytic reaction. This fact was expected to enable straightforward conclusions on the details of the catalytic cycle as well as on the intricate details of the mechanism of stereoselection. However, the real situation has proved to be much more complicated than the idealized expectations. There is a large number of experimentally characterized intermediates of Rh-catalyzed asymmetric hydrogenation. Nevertheless, neither of the possible mechanistic routes for this reaction is so far commonly accepted, whereas the new experimental results demonstrating the limits of straightforward interpretations continue to appear regularly.¹⁷

Hence, we were interested in probing the mechanism of asymmetric hydrogenation catalyzed by **5** in order to collect the additional data on the intermediates and particular steps of Rh-catalyzed asymmetric hydrogenation. Moreover, additional

(15) Gridnev, I. D.; Yasutake, M.; Imamoto, T.; Beletskaya, I. P. *Proc. Natl. Acad. Sci. U.S.A.* **2004**, *101*, 5385.

(16) For a recent review, see: Gridnev, I. D.; Imamoto, T. *Acc. Chem. Res.* **2004**, *37*, 633.

(17) (a) Evans, D. A.; Michael, F. E.; Tedrow, J. S.; Campos, K. R. *J. Am. Chem. Soc.* **2003**, *125*, 3534. (b) Drexler, H.-J.; Baumann, W.; Schmidt, T.; Zhang, S.; Sun, A.; Spannenberg, A.; Fischer, C.; Buschmann, H.-J.; Heller, D. *Angew. Chem., Int. Ed.* **2005**, *44*, 1184. (c) Reetz, M. T.; Meiswinkel, A.; Mehler, G.; Angermund, K.; Graf, M.; Thiel, W.; Mynott, R.; Balckmond, D. G. *J. Am. Chem. Soc.* **2005**, *127*, 10305.

interest was warmed by the dimeric structure of **5**: the asymmetric hydrogenation results shown in Table 1 implied that the possibility of numerous isomers for each of the intermediates does not affect strongly the excellent enantioselectivity that is characteristic of the structurally similar *P*-stereogenic BisP* ligands.

Similarly to all catalytic precursors studied previously, the removal of the diene ligands from **5** was accomplished by hydrogenation of a CD₂Cl₂ solution of **5** at -20 °C. However, there were no sharp signals attributable to a solvate complex in the NMR spectra of the resulting solution. Even if the sample was thoroughly degassed in a vacuum, only a very broad signal in the ³¹P spectrum was detected, whereas no hydride signals were found in the ¹H NMR spectrum. On the other hand, further hydrogenation of this sample (10 min at -70 °C) led to the quantitative and stereoselective formation of a dirhodium tetrahydride species (**6a**) (Figure 3, Scheme 2), which follows from the high symmetry of its ¹H and ³¹P NMR spectra.

The tetrahydride species **6a** is stable up to 0 °C (the retention of hydrogen has been monitored by checking the 1:1 ratio of the PF₆⁻ and R₃PRh signals in the ³¹P NMR spectrum of **6a**); at higher temperatures **6a** gradually decomposes without yielding any definite product. The chemical shifts (-8.22 and -15.80 ppm) of the two couples of hydride protons correspond to their axial and equatorial positions, respectively; the large coupling constant ²J_{PH} = 95 Hz (confirmed by the heteronucleus correlation experiment) of the lower field shifted hydrides attests for their *trans*-disposition with respect to one of the phosphorus atoms.

We attempted to distinguish experimentally between the four isomers **6a–d** with a symmetry corresponding to the observed ¹H and ³¹P NMR spectra (Scheme 3). However, the data obtained in the low-temperature NOE experiments were inconclusive, probably due to the relayed NOEs. Hence, we challenged this problem computationally by optimization of the structures of **6a–d** at the B3LYP/SDD level of theory (Scheme 3). The isomers **6c,d** have the axially disposed solvent molecule coordinated in the inner side of the molecule. Their significant relative instability with respect to **6a,b** is explained by the unavoidable close contacts of the solvent molecule and the bridging ethylene group. On the other hand, **6a** is slightly more stable than **6b**; apparently the equatorially coordinated molecule of CH₂Cl₂ can better accommodate the bridging ethylene group (in **6a**) than the *t*-Bu group (in **6b**). Therefore, the computational results for the tetrahydride complexes **6a–d** suggest that the bridging ethylene group in **5** provides significantly stronger hindrance than the *t*-Bu group to the axially oriented ligand, whereas in the P–Rh–P plane the hindrance created by the *t*-Bu group is slightly higher.

Thus, the hydrogenation of **5** yields quantitatively and stereoselectively a highly symmetric tetrahydride species **6a** (Figure 4). This result prompted us to study the reaction of **6a** with a prochiral substrate of asymmetric hydrogenation.

Reaction of Tetrahydride 6a with Methyl (*Z*)- α -Acetamidocinnamate. Addition of either 2 or 4 equiv of methyl (*Z*)- α -acetamidocinnamate (MAC) to the solution of **6a** in CD₂Cl₂ at -90 °C resulted in the immediate disappearance of the signals of **6a** from the NMR spectra. Instead, the clean formation of another intermediate (**7**) was observed (Figures 5, 6). By gradually raising the temperature of the sample and simultaneously checking the ratio of the PF₆⁻ and R₃PRh signals in the ³¹P NMR spectrum, we found that the intermediate **7** is stable up to approximately -40 °C. At -40 °C a slow reaction transforming **7** to a different species, **8**, begins; it is complete

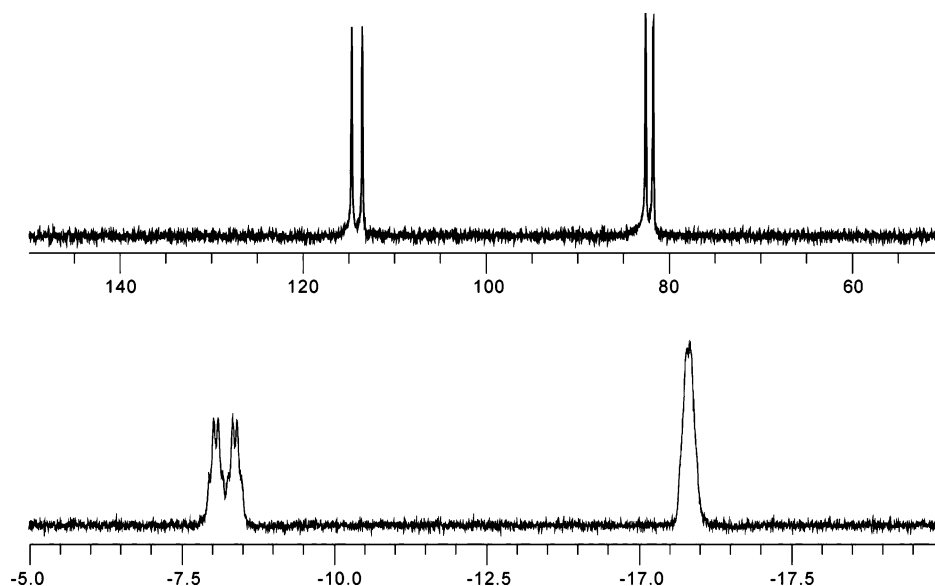
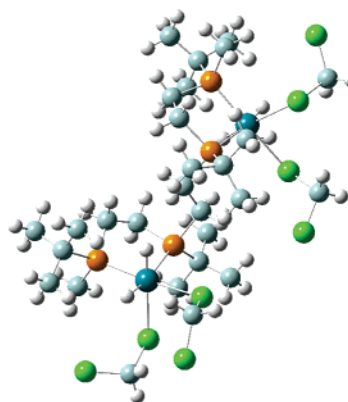
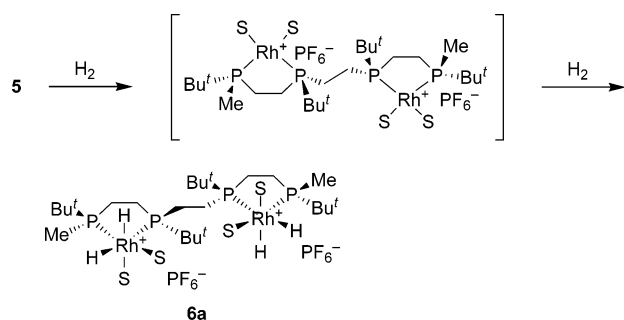
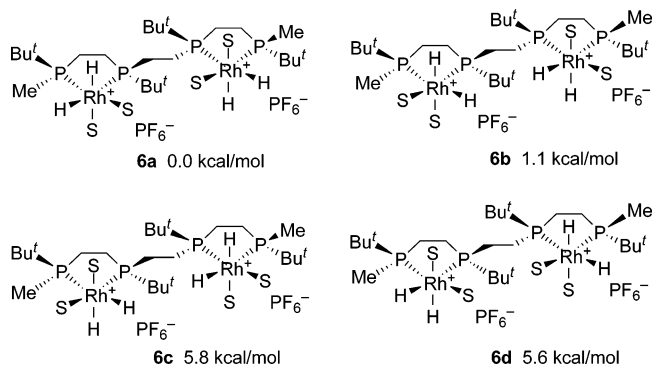


Figure 3. Section plots of ^1H NMR (300 MHz, CD_2Cl_2 , -90°C) (bottom) and ^{31}P NMR (122 MHz, CD_2Cl_2 , -90°C) (top) of the tetrahydride complex **6a**. The sum intensity of the two doublets shown in the upper plot was equal to the intensity of the multiplet from two hexafluorophosphate anions, which indicates the quantitative formation of **6a**.

Scheme 2. Formation of Tetrahydride Complex **6a**



Scheme 3. Structures of the Four C_2 -Symmetric Tetrahydrides **6a–d** and Their Relative Energies (optimized at the B3LYP/SDD level of theory)



in 30 min at -20°C . The NMR spectra of **7** and **8** are very similar; the main difference is slightly further separated signals of the hydride protons in the ^1H NMR as well as of the low-field phosphorus atoms in the ^{31}P NMR. The monitoring by multinuclear NMR showed that the whole transformation of **7** to **8** can be carried out without the appearance of appreciable amounts of the hydrogenation product (e.g., at -40°C); however, at -20°C the isomerization $7 \rightarrow 8$ is accompanied by the acquisition of the hydrogenation product. If an equivalent amount of MAC (2 equiv of MAC for 1 equiv of **6a**) has been used, the signals of **8** in the ^{31}P NMR spectrum were replaced by a very broad signal due to the solvate complex. If excessive

Figure 4. Structure of the tetrahydride complex **6a** optimized at the B3LYP/SDD level of theory. The calculations reproduce well the weakening of the Rh–P bond *trans* to the hydride ligand. The bond lengths are 2.31 Å for both Rh–P_{cis} bonds and 2.53 and 2.55 Å for the Rh–P_{trans} bonds.

MAC was present in the reaction mixture, stereoselective formation of the catalyst–substrate complex **10** was observed. If, in the presence of the excessive amount of MAC, the temperature of the sample was sharply raised to 20°C , the formation of additional intermediate **9** was detected. The structures of the intermediates **7–10** were elucidated from their spectral data and chemical properties. The intermediates **7** and **8** are slightly unsymmetrical tetrahydrides containing coordinated MAC. The manner of MAC coordination follows from the ^{13}C NMR spectra of **7** and **8**. The position and multiplicity of the CH carbon of the double bond were checked by using β - ^{13}C -labeled MAC: this carbon resonates at $\delta = 136.6$ and 129.7 in **7** and **8**, respectively, and is not coupled to either rhodium or phosphorus. Thus, the double bond in **7** and **8** remains noncoordinated. The striking difference in the ^1H chemical shifts of the amide proton of **7** ($\delta = 9.50$) and noncoordinated MAC ($\delta = 5.08$) gives reason to conclude that it is the amidocarbonyl that is coordinated to Rh. In the ^{13}C NMR spectrum of **7** the coordinated carbonyl resonates at $\delta = 178$. Reversible dynamic effects due to the chemical exchange are observed in the ^1H , ^{13}C , and ^{31}P NMR spectra of the intermediate **7**. When the temperature was gradually raised from

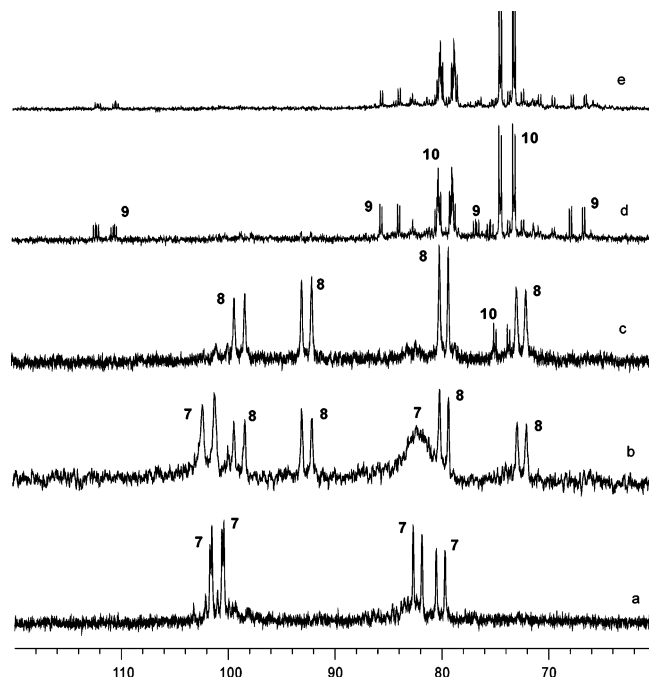


Figure 5. Evolution of the ^{31}P NMR spectrum (122 MHz, CD_2Cl_2) of the sample prepared by addition of a 4-fold excess of MAC to the solution of **6a** in CD_2Cl_2 : (a) immediately after mixing, -90°C ; (b) at -20°C ; immediately after raising the temperature; (c) at -20°C after 10 min; (d) at 20°C , immediately after raising the temperature; (e) at 20°C after 20 min.

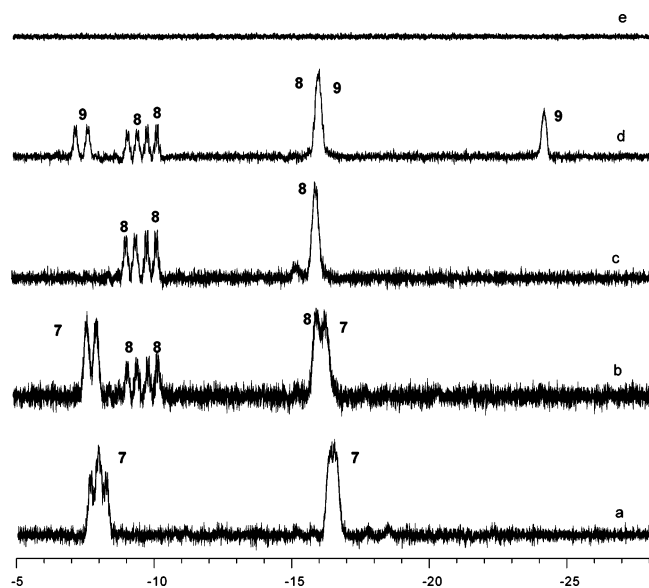
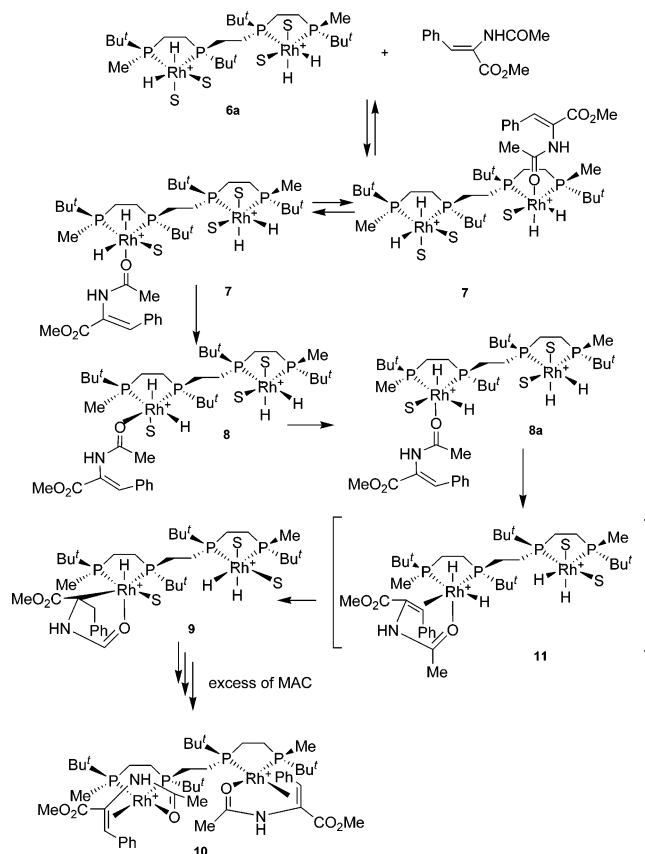


Figure 6. Evolution of the ^1H NMR spectrum (300 MHz, CD_2Cl_2) of the sample prepared by addition of a 4-fold excess of MAC to the solution of **6a** in CD_2Cl_2 : (a) immediately after mixing, -90°C ; (b) at -20°C ; immediately after raising the temperature; (c) at -20°C after 10 min; (d) at 20°C , immediately after raising the temperature; (e) at 20°C after 2 h. The enantiomeric excess of the hydrogenation product obtained after quenching of this sample was 95% ee (*R*).

-90 to -50°C , the reversible broadening of the signals in the ^{31}P NMR spectrum resulted in their collapse, indicating the occurrence of a degenerate rearrangement that makes the four phosphorus atoms of **7** equivalent in pairs. In the ^{13}C NMR spectrum of the labeled MAC the exchange of the CHPh groups of **7** and free MAC occurred with approximately the same rate as the exchange in the ^{31}P NMR. On the basis of these data we

Scheme 4. Intermediates Intercepted in the Reaction of Tetrahydride **6** with MAC



assigned the structure shown in the Scheme 4 for **7**. Only one molecule of MAC is coordinated to the dirhodium tetrahydride via its amidocarbonyl, whereas the double bond remains noncoordinated as follows from the ratio of coordinated MAC to free MAC in solution.

The spectral properties of the intermediate **8** closely resemble those of **7**. Hence, we conclude that **8** must be an isomer of **7** with the same mode of substrate coordination, but different spatial arrangement of the ligands.

The intermediate **9** is a trihydride complex with two hydride ligands in the *cis*-position to both phosphorus atoms and one hydride *trans* to phosphorus. Apparently, this is an analogue of the well-known asymmetric hydrogenation monohydride intermediates.

The catalyst–substrate complex **10** forms in the reaction mixture if an excessive amount of MAC is present. It has a symmetric structure with two MAC molecules coordinated to both rhodium atoms, as follows from the symmetry of its ^{31}P NMR spectrum (closely resembling that of **5**) and also from the number of signals in the ^1H and ^{13}C NMR spectra. The structure shown in Scheme 4 was assigned by the high-field shift of one of the *t*-Bu groups ($\delta = 0.61$) that according to the previous studies^{12b,13} indicates its vicinity to the phenyl group of the coordinated substrate. The two carbon atoms of the coordinated double bond in **10** exhibited expected values of chemical shifts and coupling constants.

The results of the study of the low-temperature reaction of **6a** with MAC allow several interesting conclusions to be made. First, quite unexpectedly and in contrast to previously studied reactions, the simultaneous presence of the Rh(III) dihydride moiety (two of them) and the substrate in the reaction mixture did not result in immediate migratory insertion. The reason for

this is that proper coordination of the double bond of MAC is impossible. The relatively small molecule of solvent acting as a ligand in **6** can more conveniently accommodate itself in the inner part of the molecule, avoiding the vicinity of the *t*-Bu groups (see above). This makes the tetrahydride **6a** more stable than **6b**, and as a result the exclusive formation of **6a** is observed. However, a quite large molecule of MAC cannot coordinate in the inner part of the molecule; therefore the interaction of **6a** with MAC gives the nonchelating complex **7** (Scheme 4). The dynamic effects in the spectra of **7** are explained by reversible dissociation of this weak complex and subsequent association of the MAC molecule to another rhodium atom of the same molecule of the catalyst (Scheme 4).

At $-40\text{ }^{\circ}\text{C}$ the isomerization of **6a** via pseudorotation¹⁸ becomes possible. When nothing except for **6a** is present in the reaction mixture, this rearrangement is not observed experimentally since **6a** is the most stable isomer among the other tetrahydrides. However, in the presence of MAC the initial binding of the amidocarbonyl in **8** or **8a** can be accompanied by the chelating coordination of the double bond across the less hindered quadrant in **11**, which results in immediate migratory insertion leading to **9**.

Conclusion

Thus, we can see that the binding of the substrate in the dihydride species directly preceding the migratory insertion step (e.g., **7** or **8**) is much weaker than the binding of the substrate in the catalyst–substrate complex (e.g., **11**). This conclusion is important, since it provides experimental support for the idea of the stereoselection during the association step of asymmetric hydrogenation that we have recently proposed in several publications.^{12b,13,15} Indeed, even if some step before the irreversible migratory insertion is stereoselective, the weak binding of the substrate in octahedral dihydride intermediates destroys the results of this stereoselection via the dissociation of the double bond. On the other hand, the fast equilibrium between all possible isomers of dihydride intermediates is facilitated by the easy dissociation of the substrate, and the whole system can swoop down the energy minimum via the single isomer of the dihydride intermediate characterized by the lowest barrier of migratory insertion. The manner in which the reaction of **6a** with MAC proceeds demonstrates how the tetrahydride species (corresponding to the dihydride intermediates in the case of monorhodium complexes) can be nonreactive if the arrangement of the ligands appropriate for the occurrence of migratory insertion is not achieved, and how they can easily interconvert in the presence of substrate, thereby opening the way for the proper coordination mode.

Straightforward interpretation of our experimental data suggests that only one diphosphine-rhodium unit out of two is participating in the hydrogenation catalytic cycle. This is a rather unexpected result, and although it might be considered as bad news from the point of view of possible future construction of polynuclear catalytic systems, it reveals the important structural restrictions for the synchronous operation of two adjacent metal centers. Apparently, when one of the rhodium atoms undergoes oxidative addition followed by coordination of the substrate, the resulting octahedral moiety creates enough hindrance to prevent coordination of the second molecule of the substrate. This must be taken into account when either polymeric or multifunctional catalytic systems are designed.

(18) (a) Berry, R. S. *J. Chem. Phys.* **1960**, *32*, 933. (b) Feldgus, S.; Landis, C. R. *J. Am. Chem. Soc.* **2000**, *122*, 12714.

Experimental Section

General Procedures. All reactions and manipulations were performed under a dry argon atmosphere using standard Schlenk-type techniques. Substrates for acymmetric hydrogenation were prepared according to the procedures described in the literature (methyl (*Z*)- α -Acetamidocinnamate,¹⁹ β,β -disubstituted dehydroamino acids,²⁰ enamides,²¹ β -dehydroamino acids,²² and α,β -unsaturated phosphonate²³) or were commercially available (dimethyl itaconate). Melting points were determined in open capillaries using a Yamato micro melting point apparatus and were not corrected. ¹H, ¹³C, ³¹P, and ¹¹B NMR spectra were recorded using JEOL AL-300, LA-400, and LA-500 instruments. Optical rotations were measured with a JASCO DIP-370 digital polarimeter with a 1-dm-long cell. Enantiomeric excesses were determined by HPLC analysis performed on a Shimadzu LC-10AD pump, Shimadzu CTO-10AC VP column oven, and Shimadzu SPD-10A VP UV detector with an appropriate chiral column. Hydrogen of 99.9999% purity (Nippon Sanso) was used for the mechanistic studies.

Preparation of Tetraphosphine-borane 3. *n*-Butyllithium (1.58 M solution) (15.4 mL, 24.4 mmol) was slowly added to a stirred, cooled ($-78\text{ }^{\circ}\text{C}$) solution of secondary diphosphine-borane **1** (2.6 g, 11.1 mmol) in THF (50 mL) under an Ar atmosphere. The solution was stirred for 2 h and then added to a stirred solution of (*R*)-*tert*-butyl(methyl)(2-(4-methylphenylsulfonyloxy)ethyl)phosphine-borane **2** (7.7 g, 24.4 mmol) in THF (50 mL). The reaction mixture was stirred for 1 h at $-78\text{ }^{\circ}\text{C}$ and for 5 h at room temperature. The reaction was quenched by addition of 1 M aqueous hydrochloric acid (100 mL). The organic layer was separated, and the aqueous layer was extracted with ethyl acetate ($3 \times 100\text{ mL}$). The combined extracts were washed with aqueous NaHCO₃ and brine and dried over Na₂SO₄. The solvent was removed on an evaporator to leave a white residue, which was recrystallized from hot toluene–hexane (2:1) to give pure **3** (65% yield) as colorless needles: mp $180\text{--}182\text{ }^{\circ}\text{C}$; $[\alpha]_{\text{D}}^{25} -4.9$ (*c* 1.0, CHCl₃); ¹H NMR (400 MHz, CDCl₃) δ 0.15–0.88 (m, 12H), 1.17 (d, $J_{\text{HP}} = 13.8\text{ Hz}$, 18H), 1.20 (d, $J_{\text{HP}} = 13.8\text{ Hz}$, 18H), 1.24 (d, $J_{\text{HP}} = 9.7\text{ Hz}$, 6H), 1.61–1.83 (m, 6H), 1.85–2.08 (m, 6H); ³¹P NMR (202 MHz, CDCl₃) δ 29.6 (d, $J_{\text{PB}} = 62\text{ Hz}$), 38.1 (br s); ¹¹B NMR (160 MHz, CDCl₃) δ -62.9 (br s), -61.0 (br d, $J_{\text{PB}} = 62\text{ Hz}$); IR (KBr) 2970, 2360, 2340 cm^{-1} ; FAB-MS (rel intensity) 521 ($\text{M}^+ - \text{H}$, 27), 491 ($\text{M}^+ - 2\text{BH}_3 - 3\text{H}$, 47), 479 ($\text{M}^+ - 3\text{BH}_3 - \text{H}$, 100), 423 ($\text{M}^+ - \text{C}_4\text{H}_9 - 3\text{BH}_3$, 38), 57 (C_4H_9 , 74).

Deboronation of Phosphine-borane 3. Tetrafluoroboric acid (solution in diethyl ether, 50 wt %) (0.98 mL, 6.9 mmol) was slowly added to a stirred, cooled ($0\text{ }^{\circ}\text{C}$) solution of tetraphosphine-borane **3** (150 mg, 0.29 mmol) in dichloromethane (10 mL) under an Ar atmosphere. After 30 min the cooling bath was removed and the reaction mixture was stirred at room temperature until the disappearance of **3** (TLC control). Then the reaction mixture was again cooled to $0\text{ }^{\circ}\text{C}$, and saturated aqueous NaHCO₃ (15 mL) was slowly added. After stirring for 30 min at $0\text{ }^{\circ}\text{C}$ and for 3 h at room temperature the reaction mixture was extracted with diethyl ether ($3 \times 30\text{ mL}$). The combined extracts were dried over Na₂SO₄, and the solution was passed through a column of basic alumina. The solvent was removed in a vacuum to give 128 mg (95% yield) of practically pure tetraphosphine **4** (white solid).

Preparation of Dirhodium Tetraphosphine Complex 5. A solution of tetraphosphine **4** (128 mg, 0.27 mmol) in freshly distilled dichloromethane (2 mL) was added to a stirred solution of [Rh-

(19) Vineyard, B. D.; Knowles, W. S.; Sabacky, G. L.; Bachman, G. L.; Weinkauff, D. J. *J. Am. Chem. Soc.* **1977**, *99*, 5946.

(20) Burk, M. J.; Gross, M. F.; Martínez, J. P. *J. Am. Chem. Soc.* **1995**, *117*, 9375.

(21) Burk, M. J.; Wang, Y. M.; Lee, J. R. *J. Am. Chem. Soc.* **1996**, *118*, 5142.

(22) Zhu, G.; Chen, Z.; Zhang, X. *J. Org. Chem.* **1999**, *64*, 6907.

(23) Burk, M. J.; Stammers, T. A.; Straub, J. A. *Org. Lett.* **1994**, *1*, 387.

(nbd)₂]PF₆ (235 mg, 054 mmol) in dichloromethane (2 mL) under an Ar atmosphere. The solution was stirred at room temperature for 3 h. Then the reaction mixture was filtered, and the solvent was removed in a vacuum. The residual solid was washed with diethyl ether to give an orange powder, which was dried in a vacuum. Recrystallization from methanol afforded 144 mg (46% yield) of **5** as red cubes: ¹H NMR (300 MHz, 293 K, CD₃OD) δ 1.05 (d, *J*_{PH} = 14 Hz, 18H), 1.11 (d, *J*_{PH} = 14 Hz, 18H), 1.38 (d, *J*_{PH} = 8 Hz, 6H), 1.61 (m, 6H), 1.86 (m, 4H), 2.0–2.7 (m, 6H), 4.10 (br. s, 2H), 4.16 (br. s, 2H), 5.62 (m, 2H), 5.84 (m, 6H); ¹³C NMR (75 MHz, 293 K, CD₃OD) δ 6.14 (d, *J*_{CP} = 23 Hz), 21.79 (m), 24.00 (m), 26.82 (d, *J*_{CP} = 26 Hz), 26.95 (d, *J*_{CP} = 26 Hz), 27.58 (m), 33.57 (m), 71.65, 73.36, 82.81 (t, *J*_{CP} = 7 Hz), 86.14 (m), 91.82 (m), 92.83 (t, *J*_{CP} = 9 Hz); ³¹P NMR (122 MHz, 293 K, CD₃OD) δ -146.0 (heptet, *J*_{PF} = 709 Hz), 63.4 (dm, *J*_{PRh} = 150 Hz), 76.3 (dm, *J*_{PRh} = 163 Hz); HR-MS (MALDI) 1252.2157 (M + 2CH₃OH + K + 3H), calcd for C₄₀H₈₁O₂F₁₂P₆Rh₂K 1252.221, proper isotopic pattern.

X-ray Data Collection. A crystal appropriate for the X-ray analysis was obtained by recrystallization of complex **5** from methanol. The intensity data were collected on a Rigaku RAXIS-II imaging plate diffractometer with graphite-monochromated Mo K α radiation. The structure was solved by direct methods and expanded using Fourier techniques. The non-hydrogen atoms were refined anisotropically. Hydrogen atoms were included but not refined. The final cycle of full-matrix was based on 3169 observed reflections (*I* > 2.00 σ (*I*)) and 541 variable parameters. Atomic coordinates, bond lengths and angles, and thermal parameters have been deposited at the Cambridge Crystallographic Data Centre.

Asymmetric Hydrogenation (General Procedure). A 50 mL Fisher-Porter tube was charged with the substrate (0.6 mmol) and the catalyst precursor (0.003 mmol). The tube was connected to the hydrogen tank via stainless steel tubing. The vessel was evacuated and filled with hydrogen gas (Nippon Sanso, 99.9999%) to a pressure of about 2 atm. This operation was repeated, and the bottle was immersed in a dry ice–ethanol bath. The upper cock of the bottle was opened, and anhydrous and degassed methanol was added quickly using a syringe. After four vacuum/H₂ cycles, the tube was pressurized to 2 atm. The solution or suspension was magnetically stirred at ambient temperature. After completion of hydrogenation (30 min) the resulting solution was passed through silica gel using ethyl acetate as the eluent, and the filtrate was submitted to direct analysis for the ee value by HPLC.

NMR Detection of Dirhodium Tetrahydride Species. Complex **5** (16 mg) was dissolved in 0.6 mL of CD₂Cl₂ under argon in a 5 mm NMR tube. The tube was connected to the Ar vacuum line and to the lecture bottle with H₂ via different stopcocks. The sample was cooled to -20 °C, and after several degassing cycles 2 atm of hydrogen was admitted. The solution in the tube was manually stirred at -20 °C under 2 atm of hydrogen for 30 min. Then the hydrogen was removed in a vacuum, and the tube was filled with argon. The NMR spectra of the thus obtained sample were recorded in the temperature interval from -100 to -20 °C. The ¹H NMR spectrum showed that the norbornadienyl ligands were completely hydrogenated, but no signals of Rh hydrides were detected in the spectral region from 0 to -40 ppm. In the ³¹P NMR spectrum a broad signal was observed with the center at 132 ppm (LW_{1/2} = 2500 Hz); its integral intensity was approximately double of that of the heptet belonging to the two PF₆⁻ anions ($\delta = -148.7$).

The sample was returned to the vacuum-gas line, and argon was removed by degassing. The sample was cooled to -70 °C, and 2 atm of H₂ was applied for 30 min. During this time the sample was stirred manually to avoid mass transfer problems. Then the sample was placed into a precooled probe of the NMR spectrometer.

Tetrahydride complex **6a**: ¹H NMR (300 MHz, CD₂Cl₂, -30 °C) δ -15.80 (m, 2H; axial hydrides); -8.22 (ddd, ²*J*_{HP^{trans}} = 95 Hz, ²*J*_{HP^{cis}}, ¹*J*_{HRh} = 22, 46 Hz); 1.19 (d, ³*J*_{HP} = 17 Hz, 18H; 2Bu^t);

1.26 (d, ³*J*_{HP} = 16 Hz, 18H; 2Bu^t); 1.68 (d, ³*J*_{HP} = 10 Hz, 6H; 2Me); 1.8–2.8 (m, 12H; 6CH₂); ³¹P NMR (122 MHz, CD₂Cl₂, -30 °C) δ = 82.2 (d, ¹*J*_{PRh} = 107 Hz), 114.1 (d, ¹*J*_{PRh} = 142 Hz).

Intermediate **7**: ¹H NMR (hydride signals, 300 MHz, CD₂Cl₂, -20 °C) δ -16.48 (m, 2H; axial hydrides); -7.96 (ddd, 2H, equatorial hydrides, ²*J*_{HP^{trans}} = 82 Hz, ²*J*_{HP^{cis}}, ¹*J*_{HRh} = 23, 45 Hz); ³¹P NMR (122 MHz, CD₂Cl₂, -20 °C) δ 80.1 (d, ¹*J*_{PRh} = 103 Hz); 82.3 (d, ¹*J*_{PRh} = 99 Hz); 101.0 (d, ¹*J*_{PRh} = 136 Hz); 101.2 (d, ¹*J*_{PRh} = 137 Hz).

Intermediate **8**: ¹H NMR (hydride signals, 300 MHz, CD₂Cl₂, -20 °C) δ -15.90 (m, 2H; axial hydrides); -10.02 (ddd, 1H, equatorial hydride, ²*J*_{HP^{trans}} = 104 Hz, ²*J*_{HP^{cis}}, ¹*J*_{HRh} = 25, 47 Hz); -9.26 (ddd, 1H, equatorial hydride, ²*J*_{HP^{trans}} = 108 Hz, ²*J*_{HP^{cis}}, ¹*J*_{HRh} = 21, 43 Hz); ³¹P NMR (122 MHz, CD₂Cl₂, -30 °C) δ = 82.2 (d, ¹*J*_{PRh} = 107 Hz), 114.1 (d, ¹*J*_{PRh} = 142 Hz); ³¹P NMR (122 MHz, CD₂Cl₂, -20 °C) δ 72.3 (d, ¹*J*_{PRh} = 107 Hz); 79.6 (d, ¹*J*_{PRh} = 102 Hz); 92.5 (d, ¹*J*_{PRh} = 116 Hz); 98.8 (d, ¹*J*_{PRh} = 119 Hz).

Intermediate **9**: ¹H NMR (hydride signals, 300 MHz, CD₂Cl₂, 20 °C) δ -24.11 (m, 1H; axial hydride); -16.00 (m, 1H; axial hydride); -7.46 (ddd, 1H, equatorial hydride, ²*J*_{HP^{trans}} = 134 Hz, ²*J*_{HP^{cis}}, ¹*J*_{HRh} = 16, 27 Hz); ³¹P NMR (122 MHz, CD₂Cl₂, 30 °C) δ 67.1 (dd, ¹*J*_{PRh} = 150 Hz, ²*J*_{PRh} = 26 Hz); 75.9 (ddd, ¹*J*_{PRh} = 160 Hz, ²*J*_{PRh} = 37 Hz, ²*J*_{PRh} = 26 Hz); 84.7 (dd, ¹*J*_{PRh} = 203 Hz, ²*J*_{PRh} = 24 Hz); 111.4 (ddd, ¹*J*_{PRh} = 200 Hz, ²*J*_{PRh} = 37 Hz, ²*J*_{PRh} = 24 Hz).

Catalyst–substrate complex **10**: ¹H NMR (300 MHz, CD₂Cl₂) δ 0.61 (d, ³*J*_{HP} = 15 Hz; 6CH₃); 1.05 (d, ³*J*_{HP} = 14 Hz; 6CH₃); 1.38 (d, ²*J*_{HP} = 9 Hz; 2CH₃); 2.00 (s; 2CH₃CON); 1.9–2.5 (m; 6CH₂); 3.72 (s; 2CH₃O); 5.91 (m; 2CH=); 6.9–7.5 (m; 2C₆H₅); ¹³C NMR (75 MHz, CD₂Cl₂, 30 °C) δ 8.4 (d, ¹*J*_{CP} = 27 Hz; 2Me); 20.6 (dd, ¹*J*_{CP} = 24 Hz, ²*J*_{CP} = 7 Hz; 2CH₂); 22.6 (d, ¹*J*_{CP} = 24 Hz, 2CH₂); 23.9 (s; CH₃CONH); 24.4 (m; 2CH₂); 26.6 (d, ²*J*_{CP} = 3 Hz, 6CH₃); 29.1 (d, ²*J*_{CP} = 3 Hz, 6CH₃); 31.4 (dd, ¹*J*_{CP} = 18 Hz, ²*J*_{CRh} = 3 Hz; 2C^{tert}); 31.8 (dd, ¹*J*_{CP} = 16 Hz, ²*J*_{CRh} = 4 Hz; 2C^{tert}); 54.0 (s, OMe); 81.9 (d, ²*J*_{CP} = 13 Hz; C β); 82.3 (dd, ²*J*_{CP} = 13 Hz, ¹*J*_{CRh} = 8 Hz); 129.3, 130.4, 130.9 (3 CH arom.); 138.2 (d, ³*J*_{CP} = 2 Hz); 168.4 (d, ²*J*_{CRh} = 4 Hz; O=C=O); 185.8 (d, ²*J*_{CRh} = 3 Hz; N=C=O); ³¹P NMR (122 MHz, CD₂Cl₂, 30 °C) δ 73.7 (dm, ¹*J*_{PRh} = 163 Hz); 79.4 (dm, ¹*J*_{PRh} = 166 Hz).

Computational Details. Geometries of all stationary points were optimized using analytical energy gradients of self-consistent-field²⁴ and density functional theory (DFT).²⁵ The latter utilized Becke's three-parameter exchange–correlation functional²⁶ including the nonlocal gradient corrections described by Lee–Yang–Parr (LYP),²⁷ as implemented in the Gaussian 03 program package.²⁸ All geometry optimizations were performed using the SDD basis set.²⁹

Acknowledgment. This research was supported by a Grant-in-Aid for Scientific Research from the Ministry of Education, Culture, Sports, Science and Technology and the Chemistry COE program of Tohoku University. The computational results in this research were obtained using supercomputing resources at Information Synergy Center, Tohoku University.

Supporting Information Available: Cartesian coordinates of the optimized structures **6a–d**; full ref 28. This material is available free of charge via the Internet at <http://pubs.acs.org>.

OM050759P

(24) Pulay, P. In *Modern Theoretical Chemistry*; Schaefer, H. F., Ed.; Plenum: New York, 1977; Vol. 4, p 153.

(25) Parr, R. G.; Yang, W. *Density Functional Theory of Atoms and Molecules*; Oxford University Press: New York, 1989.

(26) Becke, A. D. *J. Chem. Phys.* **1993**, *98*, 5648.

(27) Lee, C.; Yang, W.; Parr, R. G. *Phys. Rev. B* **1988**, *37*, 785.

(28) Frisch, M. J.; et al. *Gaussian 03*, Revision B.05; Gaussian, Inc.: Pittsburgh, PA, 2003.

(29) Leininger, T.; Nicklass, A.; Stoll, H.; Dolg, M.; Schwedtfeger, P. *J. Chem. Phys.* **1996**, *105*, 1052.